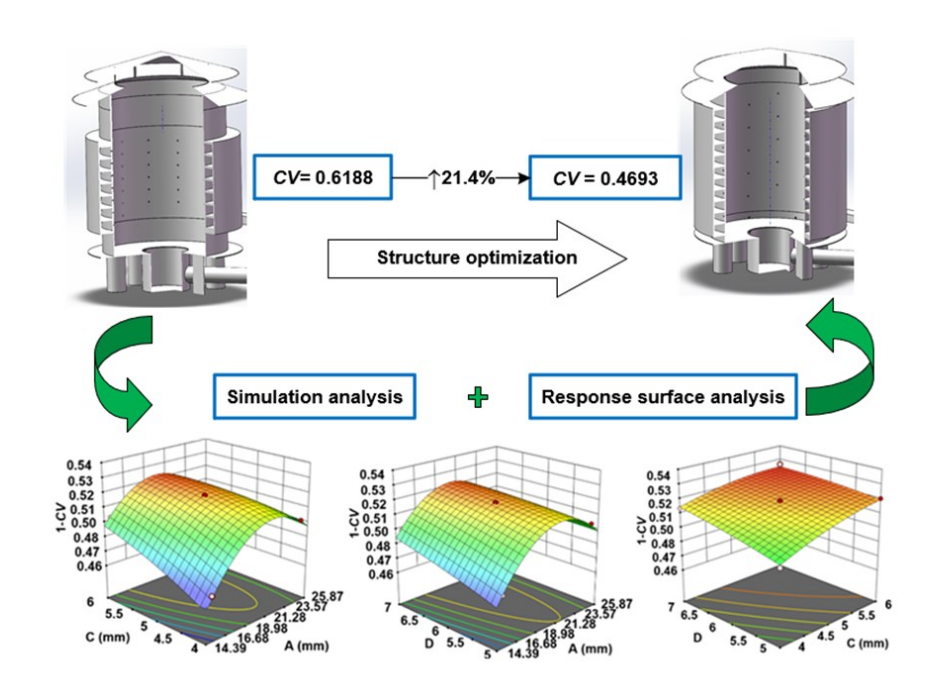
Structural Optimization of Corn Circulating Ventilator for Grain Storage Silo Based on CFD

Siyu Chen, Xi Wang, Xiaoyang Zhang, and Chunshan Liu *

* Corresponding author: liuchunshan 2001@163.com

DOI: 10.15376/biores.21.1.420-438

GRAPHICAL ABSTRACT



Structural Optimization of Corn Circulating Ventilator for Grain Storage Silo Based on CFD

Siyu Chen, Xi Wang, Xiaoyang Zhang, and Chunshan Liu *

This study optimized the ventilation structure of a fan-driven corn circulating grain storage bin. By combining computational fluid dynamics, orthogonal experiments, and response surface optimization experiments, the internal airflow field of the corn circulating ventilation of grain storage bin was simulated and the structural parameters were optimized using Fluent simulation. The optimization function of the Design-expert 13 software was utilized to determine the optimal parameter combination as follows: the diameter of the circulating inlet was 20 mm, the number of circulation layers is 13, the diameter of the bottom ventilation opening was 6 mm, and the number of ventilation openings was 7. Using the evaluation index of relative standard deviation CV, the wind speed uniformity of the storage area before and after optimization was compared. After optimization, the relative standard deviation CV of the internal flow field of the grain storage bin increased by 24.1% compared to the initial ventilation structure of the bin. This study provides important data for the optimization of the ventilation structure of corn grain storage.

DOI: 10.15376/biores.21.1.420-438

Keywords: Circulation ventilation; Uniformity of the airflow field; Structural optimization; Numerical simulation; Response surface analysis; Warehouse ventilation

Contact information: College of Mechanical Engineering Jiamusi University, Jiamusi 154007, China; *Corresponding author: liuchunshan 2001@163.com

INTRODUCTION

Post-harvest loss of grain is a global issue. Due to the limitations of storage facilities and grain storage conditions, pests, mold, and rodents have a significant impact on grain storage. Every year, 8% to 14% of the global grain output is lost during the post-harvest stage (Gao *et al.* 2016). Ventilation is an important means to ensure the quality of grain. It can regulate the gas and humidity in the grain storage, reduce mold and spoilage, inhibit mold and pests, and extend the shelf life of grain. Scientific and effective ventilation is crucial to ensuring the quality and safety of grain (Wang *et al.* 2022).

At present, the common types of grain storage facilities include flat warehouses, shallow round silos, and vertical silos. For the ventilation of grain storage facilities, two ventilation methods are generally used: transverse ventilation and longitudinal ventilation. When comparing the two types of grain storage facilities, namely shallow round silos and high flat warehouses, the transverse ventilation method has been found to be more effective than the longitudinal ventilation method for the ventilation of grain piles (Qi *et al.* 2019; Yu *et al.* 2020; Wang *et al.* 2020). Moreover, adding branch air ducts to the ventilation ducts can improve the ventilation effect of the grain silo to a certain extent (Nwaizu and Zhang 2021), but as the number of branch air ducts increases, the ventilation dead zones are not completely eliminated, and excessive turns in the branch air ducts may even reduce

the ventilation efficiency (Li et al. 2023). Yu et al. (2019) compared and analyzed the ventilation effects of various air ducts in shallow round silos, and the results showed that the combined ventilation ducts provided more uniform ventilation and better moisture reduction effects.

The ventilation process in grain silos is a highly complex process. Early studies relied on full-scale experiments and empirical models (Garg and Maier 2006), which, although practical in specific scenarios, have limited understanding of internal airflow and lack general applicability. Furthermore, such experimental processes are time-consuming, labor-intensive, and costly. Other studies have employed simplified analytical models to solve partial differential equations using methods such as the finite difference method (FDM) (Yan et al. 2015; Wei et al. 2021). Although these models are based on physical principles, they often simplify three-dimensional problems into one-dimensional or twodimensional ones, making it difficult to reveal the detailed flow mechanisms within the system. In recent years, Computational Fluid Dynamics (CFD) has emerged as a powerful tool for studying ventilation processes in granaries (Liu et al. 2020). Through numerical simulation, the airflow, temperature, and moisture changes within the grain pile can be analyzed with high accuracy, revealing the heat and mass transfer mechanisms of the grain during storage (Garg and Maier 2006; Kaimin et al. 2006; Wang et al. 2019; Zhao et al. 2023). By optimizing the ventilation duct system through simulation, the storage effect of the grain can be significantly improved (Luo 2020; Liang et al. 2021). Moreover, the simulation results of the velocity field as well as the temperature and humidity fields are usually used as important criteria for evaluating the ventilation performance (Abbouda et al. 1992). Based on this, the ventilation effect and economic benefits of the grain warehouse can be analyzed and evaluated, and the influence of different factors on the ventilation drying process can also be analyzed to determine the optimal ventilation conditions. (Yang et al. 2024, Wu et al. 2024)

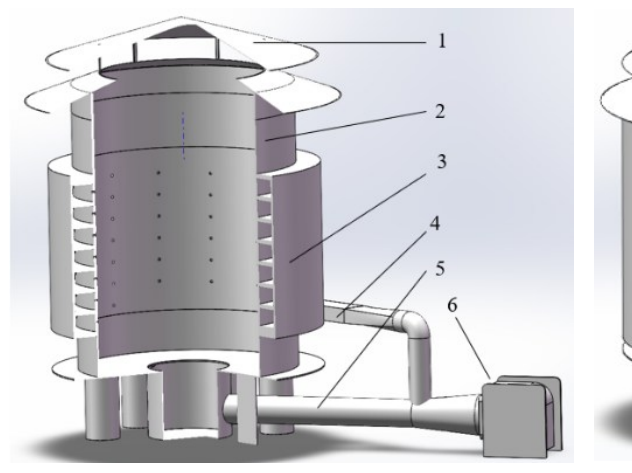
Researchers have conducted extensive studies on cross and longitudinal ventilation techniques for different silo types. Currently, the circulation technology methods mainly have focused on large-scale flat storage warehouses. There has been relatively less research on vertical silos for storing grains. The existing problems mainly lie in the uniformity of ventilation and the presence of ventilation dead zones (Qi *et al.* 2019). This paper takes corn as the research object. Based on the initial circulation ventilation storage silo scheme, Computational Fluid Dynamics (CFD) was used to simulate the distribution of the air flow field inside the silo during ventilation. Single-factor experiments were conducted to explore the factors affecting the distribution and their levels. The orthogonal test and response surface optimization methods were combined to analyze the impact of different structural parameters on the uniformity of ventilation. Design-expert 13 was used to analyze the simulation data, and the optimal parameters of the ventilation structure were obtained, providing support for the subsequent optimization of the ventilation structure of the storage silo.

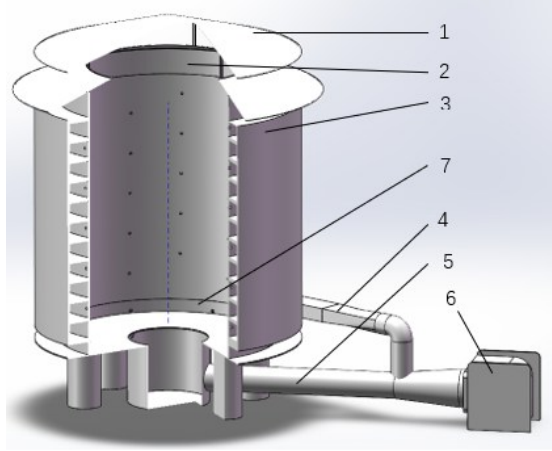
EXPERIMENTAL

Circular Ventilation Grain Storage Silo Structural Design

The main components of the storage bin in this study include the grain storage system, the circulating ventilation system, the longitudinal ventilation system, and the control system. The structure of this bin is divided into two parts: The upper part is the conical air zone, and the lower part is the cylindrical grain storage area (the wall section of the bin). The overall outer diameter of the model is 1.0 m, and the total height is 1.4 m. Among them, the diameter of the bin wall is 0.8 m, and the height is 1.2 m. The actual grain storage height is 1.0 m. Holes are opened at the bin wall to connect the circulating ventilation ducts, and a longitudinal duct with a diameter of 300 mm is set in the center of the bin bottom, with a filtering wind screen added on top to prevent grain leakage.

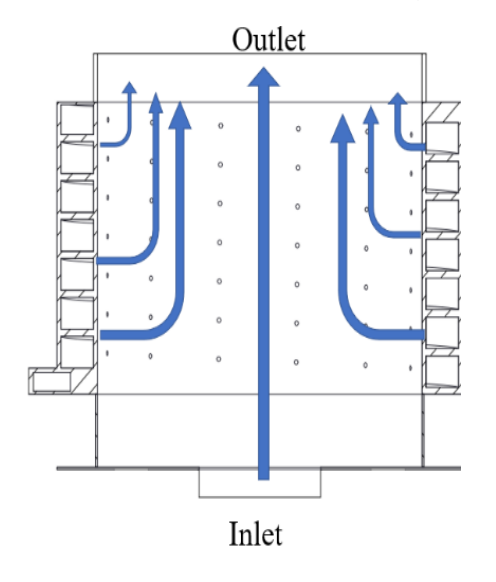
The grain storage bin model was established using the Solidworks 2022 software (Fig. 1a). The model was appropriately simplified, and the fluid domain was extracted using SpaceClaim software in ANSYS 2023. Subsequently, the model was imported into the FluentMeshing module of Fluent software for unstructured meshing of the fluid domain.

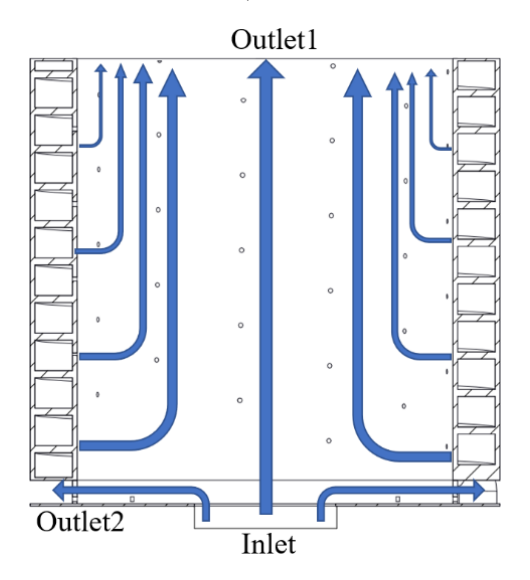




- (a) Model of the circulating ventilation grain storage silo
- (b) Model of the circulating ventilation grain storage silo

(1. Silo top; 2. Silo outer wall; 3. Circulation air duct; 4. Circulation air duct entrance; 5. Longitudinal air duct entrance; 6. Blower; and 7 Bottom air outlet)





- (c) Original scheme ventilation principal diagram
- (d) Optimized grain storage ventilation schematic diagram

Fig. 1. Model and optimization schematic of grain silo ventilation structure

Boundary Condition Setting

When ventilating the grain storage bin, the fan sends the airflow through the total air intake pipe into the longitudinal ventilation system and the circulating ventilation system respectively. Then, through the circulating air duct, the airflow diffuses in the grain layer at the outlet of the wall of the bin and the bottom outlet of the longitudinal air duct. Finally, it is discharged from the top of the bin, as shown in Fig. 1c.

For the boundary condition setting of the fluid domain model, a velocity inlet is used for the inlet, with air at a temperature of 20.0 °C and humidity of 0.007 kg/kg being supplied. The outlet is set as a pressure outlet condition because it directly connects to the external environment, with the static pressure being the standard atmospheric pressure. For the outer wall of the system, it is defined as an adiabatic and no-slip wall boundary, ignoring the heat exchange effect between the solid wall surface and the outside world. In terms of solver configuration, the coupled algorithm based on pressure-velocity coupling is selected for numerical simulation.

The flow state of a fluid is typically determined by the critical Reynolds number, $Re = \rho v/\mu$. When mechanical ventilation is performed, the gas density between pores is $\rho = 1.177 \text{ kg/m}^3$, and the fluid's viscosity coefficient is $\mu = 1.85 \times 10^{-5} \text{ Pa·s}$. The calculated minimum Reynolds number (19086) is greater than 2000, so it can be determined that the flow state of the gas inside the ventilation duct is turbulent flow. However, the pore size inside the grain pile is no greater than the product of porosity and the equivalent diameter of the grain particles, *i.e.*, $D = D_p$, resulting in a Reynolds number Re = 613 < 2000 at the location of maximum wind speed. Therefore, the gas flow within the grain layer is laminar.

The standard wall k-epsilon equation model is used for turbulence calculation, which solves the turbulent kinetic energy and its dissipation rate transport equations to close the Reynolds-averaged N-S equation system. During the calculation process, the second-order upwind scheme is used for spatial discretization to ensure the accuracy and stability of the numerical solution.

Numerical Simulation Mathematical Model

Porous media model

A porous medium is composed of a solid material framework and numerous tiny pores that are densely grouped and separated by the framework. The grain pile is formed by the aggregation of corn particles, and there are continuous pores within the grain pile, so it is regarded as a porous medium (Gong *et al.* 2021).

In the simulation calculation of the ventilation process, to simplify the computation, certain physical quantities are assumed as follows:

- 1. The grain pile inside the warehouse is considered an isotropic porous medium, with uniform airflow within the pores. And the initial grain pile has uniform moisture content.
- 2. This simulation does not involve energy exchange or component transfer; the fluid medium under study is treated as an ideal, incompressible, and steady flow.
- 3. The conservation equations, specifically the mass conservation equation and the momentum conservation equation, are followed during the simulation calculations.

In this study, the grain pile is treated as a simple isotropic and homogeneous porous medium model, and thus the model can be simplified as follows,

$$S_i = -\left(\frac{\mu}{\alpha}v_j + C_2 \frac{\rho_\alpha}{2} \mu |v| v_j\right) \tag{1}$$

where S_i is momentum source term; D_p is the average diameter of the corn particles, which is taken as 7.82 mm; θ is the porosity of the corn grain pile, which is taken as 0.411(Cheng et al. 2024); v_j is the velocity in the j direction (m/s); i and j represent the directions of the grid; v is the average velocity of the grid (m/s); α is the viscous resistance; C_2 is the inertia resistance factor, and the calculation formula is:

$$\alpha = \frac{D_{p}^{2}}{150} \frac{\theta^{3}}{(1-\theta)^{2}} \tag{2}$$

$$C_2 = \frac{3.5}{D_p} \frac{(1 - \theta)}{\theta^3} \tag{3}$$

From this, the coefficient of viscous resistance is calculated as follows: $D = \frac{1}{\alpha} = 1.22569631 \times 10^7 \,\text{m}^{-2}$. The inertial resistance coefficient, C_2 , is 3797.1 m⁻¹.

Continuity equation:

The model requires continuity, as defined in Eq. 4:

$$\nabla v = 0 \tag{4}$$

Momentum equation

The momentum conservation equation states that in a control volume, the rate of change of the fluid momentum over time is equal to the resultant external force acting on that control volume (Yang *et al.* 2022). The momentum conservation is expressed using Eq. 5:

$$\frac{D\vec{V}}{D_t} = \vec{f} - \frac{1}{\rho} \nabla p + \frac{\mu}{\rho} \nabla^2 \vec{V} + \frac{1}{3} \frac{\mu}{\rho} \nabla (\nabla \vec{V})$$
(5)

In Eq. 5, ρ is density at that point (kg/m³); p stands for pressure (Pa); f is the mass force, (m/s²); V is the vector velocity (m/s); and μ is the dynamic viscosity (Pa•s).

Standard k- ε equation

$$\nabla \cdot (\rho v k) = \nabla \cdot \left(\frac{\mu_{\text{eff}}}{\sigma_k} \cdot \nabla k\right) + G_k - \rho \theta \tag{6}$$

$$\nabla \cdot (\rho v \varepsilon) = \nabla \cdot \left(\frac{\mu_{\text{off}}}{\sigma_{\varepsilon}} \cdot \nabla k \right) + \left(C_1 G_k \varepsilon - C_2 \rho \varepsilon^2 \right) / k \tag{7}$$

In Eqs. 6 and 7, G_k is turbulent kinetic energy generated by the mean velocity gradient, measured in kg/(m·s)²; ε is the turbulent dissipation rate; σ_k is the turbulent Prandtl number for turbulent kinetic energy, with a value of 1.0; σ_{ε} is the turbulent Prandtl number for the dissipation rate, with a value of 1.3; and C_1 and C_2 are empirical constants, taking values of 1.44 and 1.92, respectively (Ren *et al.* 2012).

Evaluation criteria

The relative standard deviation (CV) is a measure of relative variability and is a dimensionless value. It can be used to compare the dispersion of populations with significantly different means, and also to assess the degree of improvement in the uniformity of the flow field (Li et al. 2013):

$$CV = \frac{S}{\bar{V}} \times 100\% \tag{8}$$

$$S = \sqrt{\frac{1}{n-1} \sum_{j=1}^{n} \left(V_j - \bar{V} \right)^2}$$
 (9)

In Eqs. 8 and 9, S is standard deviation of speed; V_j is the speed at the j^{th} detection point, in m/s; \overline{V} is the average speed of all detection points (m/s); and n is the number of detection points. The uniformity of the flow field on the detection surface is evaluated by the CV value. The value of CV is inversely proportional to the uniformity of the flow field. That is, the smaller the value of CV, the higher the uniformity of the flow field. To facilitate a more intuitive evaluation of the optimization effect, (1-CV) is used for evaluation in the response surface optimization experiment. Based on the structural characteristics of the circulating bin, the grain storage section is divided into sections along the axial direction for assessment.

Initial Scheme Flow Field Simulation Analysis

Grid independence

During Fluent simulation, the speed of simulation calculations and the accuracy of simulation results are affected by the number of grids. If the number of grids is small, the accuracy of the simulation results will be relatively low and the error will be large, or the simulation may diverge and fail to converge. There is a positive correlation between the calculation accuracy of Fluent numerical simulation and the grid density, but as the grid size increases, it will significantly increase the computational resource consumption and affect the solution efficiency. This requires higher performance configuration of the computing equipment. This study determined the optimal grid partition scheme through grid independence analysis: constructing 7 different-sized grid quantities (604,000, 608,000, 666,000, 815,000, 1,056,000, 1400,000, 1,747,000). This enabled analysis of the variation laws of pressure field and velocity field parameters of the grain warehouse outlet characteristic section with grid densification. As shown in Fig. 2, when the grid quantity exceeds the one million level, the fluctuation range of pressure and velocity parameters stabilizes within 0.5%, which can meet the simulation requirements. Based on the comprehensive consideration of calculation accuracy and efficiency, the optimal grid quantity for model calculation is finally selected as 1,056,000 (Zhu et al. 2023).

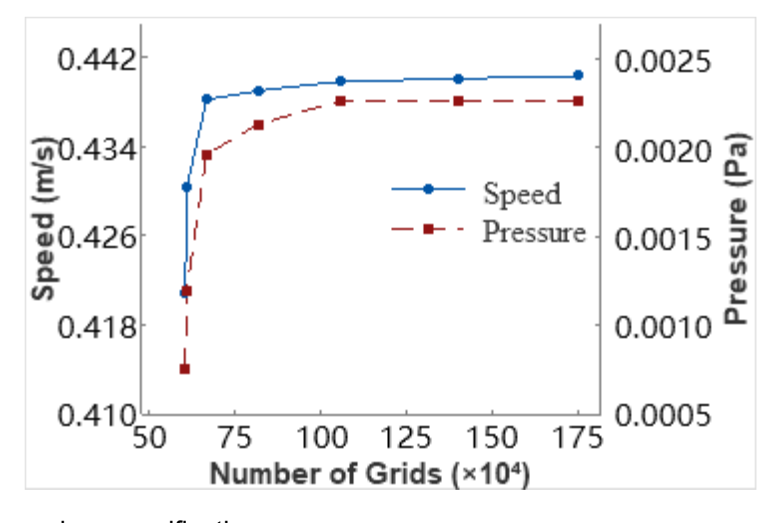


Fig. 2. Grid independence verification

To further optimize the circulating grain storage bin, a test bin was constructed at a 1:1 scale based on the original model, as shown in Fig. 3. A DPT15-34 type fan with a power of 52 W and a wind volume of 0~500 m³/h was used for ventilation tests. The XY-MD02 type 485 communication temperature sensor was used to measure the temperature at 15 monitoring points in the test bin, with data being statistically recorded every 5 min. The average temperature of the incoming grain was 21.25 °C, and the environmental temperature was 20.00 °C. After turning on the fan, the cold air was sent into the grain pile through the bottom longitudinal air duct and the circulating air duct, and the changes in the temperature of different grain layers and the overall average temperature after 1.0 h of ventilation were obtained, as shown in Fig. 4.



Fig. 3. Circulation ventilation test chamber

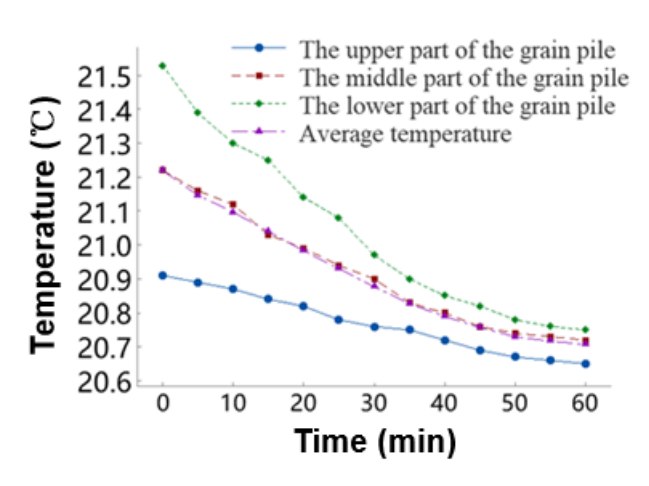


Fig. 4. Temperature changes of each grain layer in the initial granary model

The initial scheme model (with a circulating air outlet diameter of 10 mm and 7 layers of circulating air ducts) was simulated. The velocity contours of the storage section at the YX interface of the grain pile and the cross-sectional velocity cloud diagram of the grain pile inlet were selected to observe the distribution of the gas flow velocity cloud in the porous medium of the grain layer after entering the grain pile. As shown in Fig. 5. The test results indicate that after the gas flow enters the grain pile, it is affected by the resistance of the grain layer, and the gas flow velocity will gradually decrease. The closer to the outlet, the lower the wind speed. Due to the small diameter of the circulating air outlet, the gas flow enters the grain pile too quickly, resulting in a large difference in the gas flow velocity within the grain pile, which is not ideal for the uniform distribution of the gas flow in the storage warehouse. The relative standard deviation CV is large, and the overall uniformity of the flow field is poor. The original scheme has fewer circulating layers and is concentrated in the middle, having a relatively small impact on the dead zones at the top and bottom of the grain warehouse. This causes a slow cooling rate and a ventilation dead zone to form at the bottom of the storage section. Optimization is required.

Table 1. Speed and Flow Field Uniformity of the Original Scheme

Parameters	Speed (m/s)	CV Relative standard deviation	(1- CV)
	0.4890	0.6188	0.2812

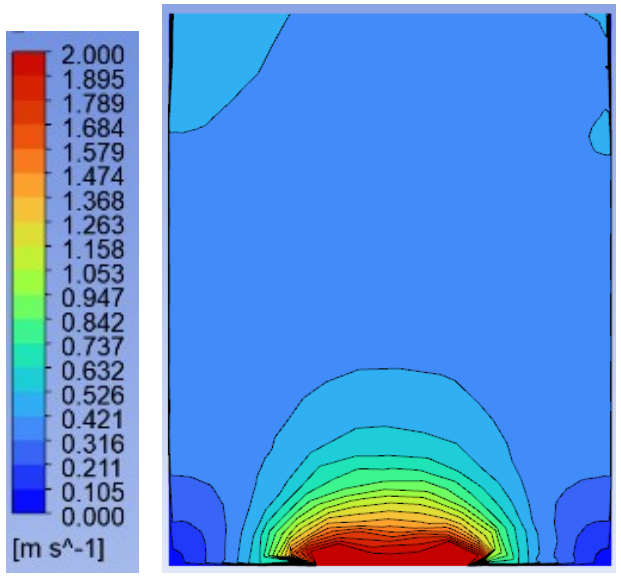


Fig. 5. Cloud map of airflow velocity at YX

Optimization of the Circulating Ventilation Grain Storage Structure

The influence of different factors on the uniformity of ventilation in grain storage facilities. The initial circulation ventilation chamber has a relatively large relative standard deviation CV, and the overall uniformity of the flow field is poor. The number of air duct layers is low, and the diameter of the air intake ports on the grain storage wall is small, concentrated in the middle, which has insufficient impact on both the upper and lower parts of the grain storage. It is necessary to appropriately increase the number of air duct layers and the diameter of the air intake ports. There are dead zones of wind speed at the corners around the bottom of the grain storage. Due to the high pressure at the bottom, adding a circulation air duct inlet at the bottom has a relatively small impact on it. Therefore, two additional air outlets are added around the bottom. Without affecting the wind speed in the middle and upper parts of the grain storage, the uniformity of the flow field in the bottom corner area is improved (as shown in Fig. 1(b)), in order to solve the problem of dead zones in bottom ventilation and poor uniformity. The optimized ventilation diagram of the grain storage facility is shown in Fig. 1(d).

To analyze the influence of different factors on the velocity field of the grain storage, single-factor experiments were conducted for four factors: the diameter of the outlet of the circulation ventilation system, the number of circulation air duct layers, the diameter of the bottom outlet, and the number of bottom outlets. The influencing factors and the range of orthogonal test levels were determined.

Inlet diameter of the circulation air duct

The diameter of the circulating air inlet affects the wind speed inside the grain pile. If the airflow enters the grain pile too quickly or too slowly, it causes a significant difference in the wind speed within the grain pile, which affects the uniformity of the airflow inside the circulating ventilation grain storage bin. Based on the actual conditions, the diameter range of the outlet of the circulating ventilation system is set as 10, 20, 30, 40, and 50 mm. The inlet wind speed is 3 m/s, the diameter of the bottom outlet is 5 mm, the number of bottom outlets is 6, and the number of layers of the circulating air duct is 12.

Under these conditions, simulation calculations were carried out to obtain the changes in data such as the average speed and the relative standard deviation CV inside the grain storage bin, as shown in Table 2.

Table 2. Influence of the Outlet Diameter of the Circulating Ventilation System

Diameter of the Circulation Air Inlet (mm)	10	15	20	25	30
Wind speed (m/s)	0.4932	0.4869	0.4766	0.4778	0.4706
CV	0.6516	0.5317	0.4746	0.5154	0.6633

From Table 2, it can be seen that in the laminar flow field of the grain flowing in the circular air duct, as the diameter of the outlet of the circular ventilation system increases, both the average flow velocity and CV show a decreasing trend. This is mainly attributable to the increase in the aperture size of the intake duct, the increase in surface area, and the increase in the amount of air participating in the distribution, thereby improving the distribution of air. When the diameter is 10 mm, the CV of the wall of the silo is very large, and the flow on the entire silo wall is not uniform. However, this situation improves as the pipe diameter increases; when the diameter of the circular intake duct increases to 20 mm, the reduction in the average flow velocity and the relative standard deviation CV gradually decreases. This indicates that the marginal effect of increasing the diameter of the circular intake duct on improving the uniformity of the flow field is gradually decreasing. Therefore, the range of the diameter of the circular inlet is determined to be $15\sim25$ mm.

Number of circulation air duct layers

In order to analyze the influence of different numbers of layers of the circulating air duct on the uniformity of the airflow field within the grain pile, this study sets the number of layers of the circulating air duct as 10, 11, 12, 13, and 14 respectively. The inlet wind speed is 3 m/s, the diameter of the bottom outlet is 5 mm, the number of bottom outlets is 6, and the diameter of the circulating inlet is 20 mm. Simulation calculations are carried out under these conditions to obtain the changes in data such as the average velocity and uniformity index within the grain warehouse, as shown in Table 3.

Table 3. Influence of the Number of Circulating Air Duct Layers

Number of Circulation Layers	10	11	12	13	14
Windspeed (m/s)	0.4825	0.4819	0.4766	0.4767	0.4773
CV	0.6578	0.5278	0.4746	0.5079	0.5141

From Table 3, it can be seen that as the number of layers of the circulation air duct increases, the average flow velocity of the air in the grain layer first decreases and then becomes stable, while the relative standard deviation CV first decreases and then increases. This is mainly because the more layers of the circulation air duct there are, the larger the surface area is, and the more air participates in the distribution, which is more beneficial to the distribution of air. When the number of circulation air duct layers is 10, the CV of the entire warehouse is very large, and its influence becomes better as the number of circulation layers increases; when the circulation layers exceed 12, the decreasing trend of the average flow velocity and the relative standard deviation CV gradually slows down. This indicates that with the increase in the number of circulation air duct layers, the improvement effect

on the uniformity of the flow field is gradually decreasing. Considering all these factors, the diameter range of the circulation air inlet is determined to be 11 to 13 layers. Diameter of the bottom exhaust outlet

Setting the bottom exhaust outlet can improve the uniformity of ventilation and the bottom ventilation dead zone. However, if the diameter of the bottom exhaust outlet is too large, it will change the wind speed of the air flow passing through the grain pile inside the storage silo, thereby affecting the uniformity of the flow field in the circulating ventilation storage silo. Based on the actual design, the diameter range of the bottom exhaust outlets is set to 4, 5, 6, 7, and 8 mm, with the inlet wind speed being 3 m/s. Under the conditions of a circulating ventilation system with an outlet diameter of 20 mm, 6 bottom exhaust outlets, and 12 layers of circulation air ducts, CFD simulation calculations are carried out to obtain the data of the average velocity and relative standard deviation CV of the detection surface inside the grain pile of the storage silo, as shown in Table 4.

Table 4. Influence of the Bottom Air Outlet Diameter on the Relative Standard Deviation and Average Velocity

Diameter of the Bottom Air Outlet (mm)	4	5	6	7	8
Wind speed(m/s)	0.4831	0.4765	0.4843	0.4808	0.4797
CV	0.5137	0.4746	0.4822	0.5182	0.5209

From Table 4, it can be seen that as the diameter of the bottom outlet increases, the average velocity and relative standard deviation CV of the airflow within the circulatory air duct after moving through the grain layer show a trend of first decreasing, then increasing, and then stabilizing. This is because the increase in the diameter of the bottom outlet leads to an increase in the outflow area, and the proportion participating in the airflow distribution increases, significantly enhancing the ability to distribute the airflow in the dead zone at the bottom of the grain pile. At the initial diameter of 4 mm, the CV in the warehouse is relatively high, and the uniformity of the internal flow field in the grain pile is poor; as the diameter increases, the uniformity of the flow field gradually improves; when the diameter reaches 5 mm, the CV begins to increase, indicating that the improvement effect of the increase in the diameter of the bottom outlet on the dead zone at the bottom of the grain pile is weakening, and the impact on the upper part of the grain warehouse increases. Considering all factors, the most favorable diameter range of the bottom outlet is determined to be $4\sim6$ mm.

Number of bottom air outlets

The number of bottom exhaust vents can improve the uniformity of ventilation and the dead zone of ventilation at the bottom. However, too many bottom exhaust vents will affect the wind speed in the grain storage section, which may subsequently affect the uniform distribution of the airflow inside the circulating ventilation grain storage bin. Based on the actual design, the number of bottom exhaust vents is set to 4, 5, 6, 7, and 8. The inlet wind speed is 3 m/s, the diameter of the circulating ventilation system exhaust vents is 20 mm, the diameter of the bottom exhaust vents is 5 mm, and the number of layers of the circulating air duct is 12. Under these conditions, CFD simulation calculations are carried out to obtain the data of the average velocity and relative standard deviation CV of the detection surface inside the grain pile of the grain storage bin, as shown in Table 5.

Table 5. Influence of the Number of Bottom Air Outlets

The Number of Bottom Air Outlets	4	5	6	7	8
Wind speed(m/s)	0.4834	0.4825	0.4766	0.4816	0.4823
CV	0.5114	0.5097	0.4746	0.4855	0.4999

From Table 5, it can be seen that when the number of bottom ventilation holes increases, the air flow velocity and the CV in the grain layer show a trend of first decreasing, then increasing, and then stabilizing. This is because the more bottom supply vents there are, the larger the area of the bottom supply vents, the more the number of supply air involved, and the more uniform the flow field of the grain pile. When the number of bottom exhaust vents is 4, the CV value is relatively large. As the number of exhaust vents increases, the uniformity of the flow field in the warehouse improves, and as the number of exhaust vents increases, this effect improves somewhat; when the number of exhaust vents reaches 6 or more, the relative standard deviation gradually increases. This indicates that the increase in the number of exhaust vents gradually reduces the effect of improving the ventilation dead zone, while enhancing the effect on the upper part of the grain pile airflow. Considering all factors, the range of bottom exhaust vent numbers is determined to be 5 to 7.

Orthogonal Experiment Analysis

Based on the above single-factor experiments, it was found that the diameter of the outlet, the number of circulation air duct layers, the diameter of the bottom ventilation opening, and the number of ventilation openings all impact the uniformity of the flow field. The orthogonal test was used to analyze the influence relationship of the parameter combinations of the four factors on the uniformity of the circulating air storage silo. Based on the results of the single-factor experiments, the range of level changes for each factor in the experiment was determined as A (circulation inlet duct diameter) 15~25 mm, B (number of circulation air duct layers) 11~13 layers, C (diameter of bottom ventilation opening) 4~6 mm, and D (number of bottom ventilation openings) 5~7. According to the selected levels of the experimental factors, the factors and level table as shown in Table 6 were determined. The L9(3⁴) orthogonal table was selected in the Design -expert software for CFD simulation calculation. The simulation scheme and results are shown in Table 7.

Table 6. Orthogonal Test Factor Levels

Lovel		Facto	or	
Level	A(mm)	В	C(mm)	D
1	15	11	4	5
2	20	12	5	6
3	25	13	6	7

Based on the physical model, boundary conditions and orthogonal test table, a CFD simulation of the ventilation process of the circulating ventilation grain storage bin model was conducted. The velocity distribution inside the grain pile of the grain storage bin and the velocity data at the detection surface were obtained. Through the Design Expert 13 software, orthogonal test analysis was carried out to obtain the range analysis results, and the degree of influence of each factor on the uniformity of the flow field was as follows: the number of ventilation outlets > the diameter of the bottom ventilation outlet > the diameter of the circulating inlet > the number of circulating layers.

Table 7. Experimental Design and Results

Experiment Number	A (mm)	В	C (mm)	D	(1- CV)
1	15	11	4	5	0.5181
2	15	12	5	6	0.4683
3	15	13	6	7	0.5309
4	20	11	5	7	0.5086
5	20	12	6	5	0.5254
6	20	13	4	6	0.4861
7	25	11	6	6	0.4857
8	25	12	4	7	0.4840
9	25	13	5	5	0.5043
K1	0.5058	0.5042	0.4961	0.5159	
K2	0.5067	0.4926	0.4938	0.4801	
K3	0.4913	0.5071	0.5140	0.5078	
R	0.0153	0.0145	0.0202	0.0359	
Optimal solution	A2	В3	C3	D1	
Primary and secondary factors			D>C>A>B		

Response Surface Optimization Experiment

To improve the optimization accuracy, based on the results of the orthogonal experiment, factor B (the number of layers of the circulating air duct) has the least impact on (1-CV). Therefore, the top three factors A, C, and D with greater impact are selected for response surface optimization. The Box-Behnken response surface method is used to design the diameters of the inlet of the A circulation air duct, the diameters of the bottom ventilation holes of C, and the number of ventilation holes of D. A total of 15 experiments (as shown in Table 8) are conducted with 3 factors and 3 levels, and the relative standard deviation CV is calculated respectively.

 Table 8. Test Results of Response Surfaces

Experiment Number		Factor		4.01/
	A (mm)	C (mm)	D	1- <i>CV</i>
1	15	5	5	0.4788
2	25	4	6	0.5043
3	15	5	7	0.4988
4	25	6	6	0.5027
5	15	4	6	0.4735
6	25	5	7	0.5074
7	15	6	6	0.5033
8	25	5	5	0.5071
9	20	6	7	0.5307
10	20	4	5	0.4989
11	20	5	6	0.5219
12	20	6	5	0.5238
13	20	4	7	0.5162
14	20	5	6	0.5219
15	20	5	6	0.5219

The quadratic multiple regression model for the three factors based on (1 - CV) is as follows: $(1 - CV) = 0.5219 + 0.0084A + 0.0085C + 0.0056D - 0.0078AC - 0.0049AD - 0.0026CD - 0.0227A^2 - 0.0033C^2 - 0.0012D^2$. The significance test of the model: P = 0.001 < 0.05, the R^2 of the model is 0.9935, R^2_{adj} is 0.9818, and $R^2_{Predicted}$ is 0.8959. This indicates that the model is significant. The order of significance of individual factors is bottom ventilation opening diameter (C) > circulation inlet opening diameter (A) > number of outlets (D), with all P values less than 0.05 and being significant. The order of significance of the interaction between two factors is AC > AD > CD.

RESULTS AND DISCUSSION

The Influence of a Single Factor on the Uniformity of Ventilation

When the number of circulation layers is 13, under the condition that the other two factors remain unchanged, the influence of each single factor on (1-CV) is shown in Fig. 6.

In Fig. 6(a), when factors C and D remain unchanged, as the diameter of the circulation inlet of factor A increases, (1-CV) shows a trend of first increasing and then decreasing. When factor A is around 20 mm, (1-CV) is the maximum. This is because if the diameter of the outlet of the circulation duct is too large or too small, it will cause a large difference in the air flow velocity inside the grain pile, and the effect of uniform air flow distribution in the storage grain bin will not be ideal. In Fig. 6(b), when factors A and D remain unchanged, as the diameter of the bottom ventilation opening of factor C increases, (1-CV) shows a gradually increasing trend. In Fig. 6(c), when factors A and C remain unchanged, as the number of bottom ventilation openings of factor D increases, (1-CV) shows a gradually increasing trend. This is because the larger the area of the bottom supply opening of factor C or the larger the number of bottom supply openings of factor D, the greater the impact on the ventilation dead zone at the bottom of the grain pile, and (1-CV) is larger, and the uniformity of the flow field is better.

In summary, the range of factor A (circulation inlet diameter) is determined to be around 20 mm, factor C (bottom ventilation opening diameter) is determined to be around 6 mm, and factor D (number of bottom ventilation openings and circulation inlet number) is determined to be around 7.

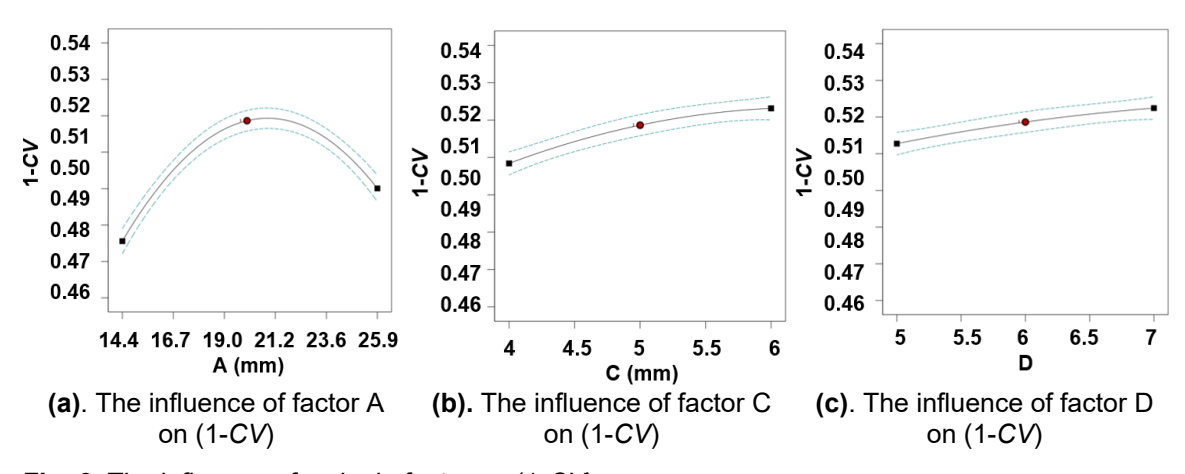


Fig. 6. The influence of a single factor on (1-CV)

The Influence of the Two Factors on the Uniformity of Ventilation

Further analysis of the influence of the two factors on (1-CV) was conducted, and the influence of the interaction effects of factors AC, AD, and CD on (1-CV) was analyzed separately, as shown in Fig. 7.

The influence of the factor AC interaction on (1-CV) is shown in Fig. 7(a): at this time, the number of ventilation outlets is 6. When the factor AC interaction occurs, the influence of factor A (circulation inlet diameter) on (1-CV) is more obvious. As factor A increases, (1-CV) first increases and then decreases; when factor A is about 20 mm, (1-CV)is at a maximum. The influence of the factor AD interaction on (1-CV) is shown in Fig. 7(b): currently, the diameter of the bottom ventilation outlet is 5 mm. When the factor AD interaction occurs, the influence of factor A (circulation inlet diameter) on (1-CV) is more obvious. As factor A increases, (1-CV) first increases and then decreases; when factor A is about 20 mm, (1-CV) is at a maximum. The influence of the factor CD interaction on (1-CV) is shown in Fig. 7(c): when the factor CD interaction occurs, at this time, the diameter of the circulation inlet is 20 mm. The influence of factors D (bottom ventilation outlet quantity) and C (bottom ventilation outlet diameter) on (1-CV) is both positively correlated. As factors C and D increase, (1-CV) continues to increase. From the above, factor A (circulation inlet diameter) is determined to be about 20 mm, factor D (bottom ventilation outlet quantity) is determined to be about 7, and factor C (bottom ventilation outlet diameter) is determined to be about 6 mm.

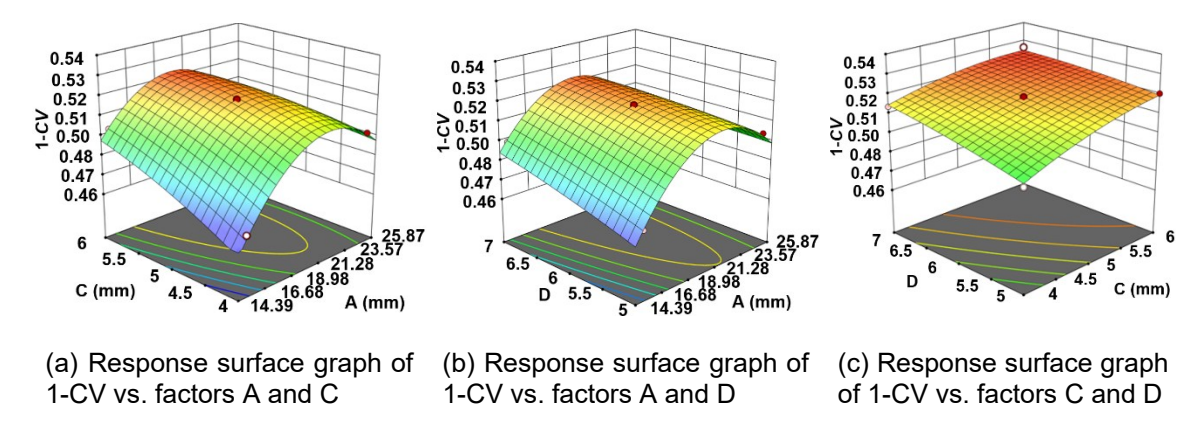


Fig. 7. The influence of two factors on (1-CV)

Optimization Plan Comparison

By utilizing the final parameter optimization prediction function of the Design-expert 13 software, aiming for the maximum (1-CV) value, the optimal parameters are obtained as follows: The number of ventilation outlets is 7.00, the diameter of the bottom ventilation outlet is 6.00 mm, and the diameter of the circulating inlet airway is 19.51 mm. Based on the actual conditions, the optimal parameter combination is determined as a circulating inlet airway diameter of 20 mm, 13 circulation layers, a bottom ventilation outlet diameter of 6 mm, and 7 ventilation outlets. To verify the effect of the optimized circulating ventilation chamber, the optimal parameter combination is used for simulation in Fluent, and the results are compared with the original structural data as shown in Table 9.

Table 9. Comparison of Schemes

Relative Standard Deviation CV	Original Plan	Optimization plan
YX section of the grain pile	0.6188	0.4693
The cross-section Y of ZX is 0.01 m	0.9646	0.9206
The cross-section Y of ZX is 0.5 m	0.15198	0.0548
The cross-section Y of ZX is 0.6 m	0.21368	0.1303

It can be seen from Table 9 that the relative standard deviation CV values of each section before and after optimization changed significantly, and they all decreased to varying degrees. The results show that the optimization effect of the circulating ventilation structure of the grain storage bin was remarkable.

Figure 8 shows the comparison of the grain pile velocity contours. Parts 8a and 8b indicate that in the original scheme, the circulating air ducts were concentrated in the middle of the grain storage bin, having a relatively small impact on the upper part of the bin, resulting in a lower wind speed at the grain pile outlet in the original scheme. The optimized grain storage bin increased the number of circulating air duct layers and strengthened the influence on the upper part of the grain pile, resulting in an increase in the wind speed in the upper part of the grain pile. For the ventilation dead zone at the bottom of the grain, appropriate diameter and quantity of outlets were added at the bottom of the grain storage bin wall to alleviate the bottom ventilation dead zone without affecting the flow field in the upper part of the bin, in order to improve the uniformity of the flow field.

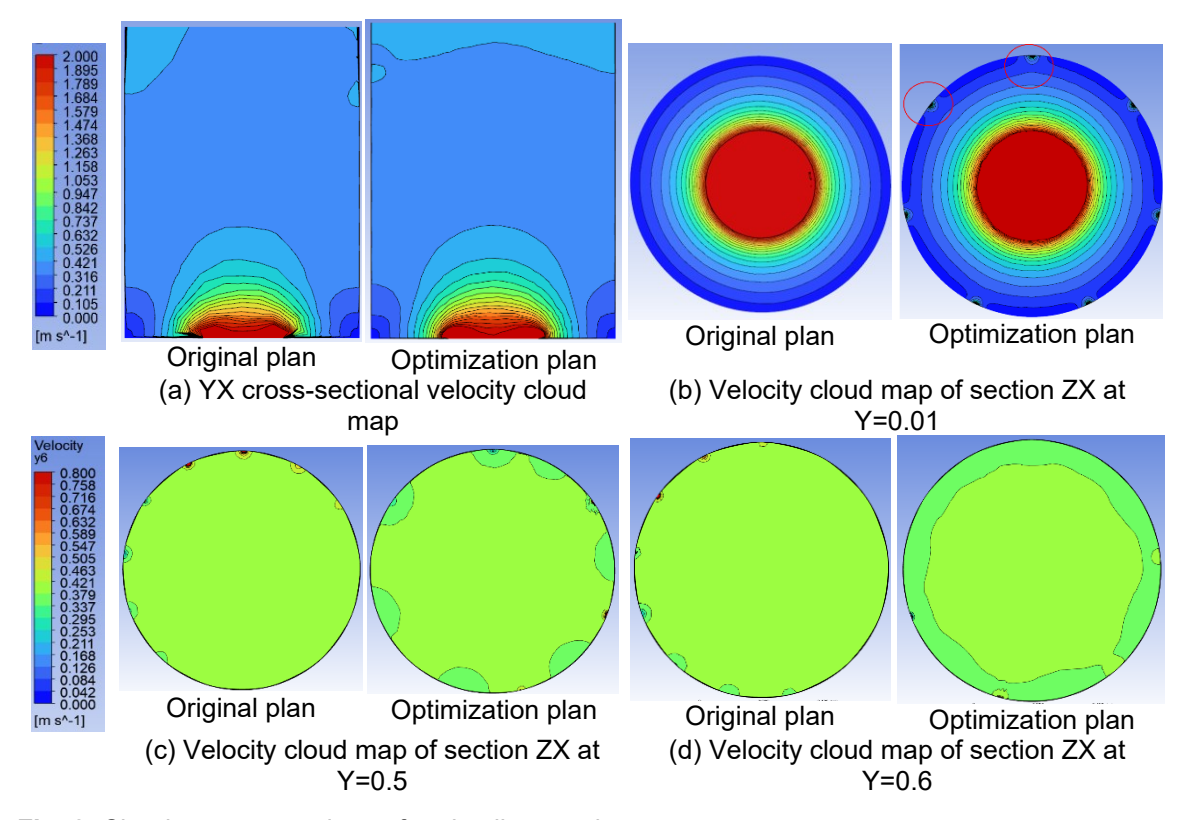


Fig. 8. Cloud map comparison of grain pile speed

Figures 8c and 8d show that due to the influence of the grain layer resistance on the airflow of the circulating ventilation bin, in the original scheme, the diameter of the

circulating air duct outlet was small, and the circulating air duct was concentrated in the middle of the grain storage bin, resulting in an excessively fast flow speed when entering the grain pile, causing a large difference in the airflow speed within the grain pile, and the effect of uniform distribution of the airflow in the grain storage bin was not ideal, resulting in poor uniformity of the flow field in the grain pile in the bin. By appropriately increasing the number of circulating air duct layers and the diameter of the circulating air duct outlets, and evenly distributing the circulating air ducts on the middle, upper, and lower parts of the bin wall, the difference in the airflow speed within the grain pile caused by the concentration of the inlet of the circulating air duct can be reduced, and the uniformity of the flow field in the middle part of the bin can be increased.

Therefore, based on the optimal parameters obtained through the Design Expert 13 software, the diameter of the outlet of the circulation duct and the number of circulation layers were appropriately increased to enhance the influence on the upper part of the grain pile, and to optimize the uniformity of the flow field in the middle part of the grain pile. The additional outlets at the bottom effectively alleviated the ventilation dead zone at the bottom of the grain pile and improved the overall ventilation uniformity of the circulation air chamber. After the optimization, the average wind speed of the circulation air chamber slightly decreased, and the relative standard deviation *CV* dropped to 0.4693. Compared with the original scheme, the uniformity index was improved by 24.1%, and the flow field uniformity was enhanced. The average wind speed in the bottom area at Y=0.01 increased from 0.799 m/s to 0.811 m/s, effectively alleviating the bottom dead zone.

CONCLUSIONS

- 1. A simulation analysis was conducted on the initial grain storage model. The results showed that the small outflow holes of the circulation air outlets led to an excessively fast air flow speed inside the warehouse, and CV increased. At the same time, the number of circulation layers was small and concentrated in the middle, which had insufficient impact on the dead zones at the top/bottom of the warehouse, resulting in a ventilation dead zone at the bottom of the warehouse and poor uniformity of the flow field (CV = 0.6188). Therefore, orthogonal experiments and response surface methods were used to optimize the ventilation structure to improve uniformity, eliminate dead zones, and enhance efficiency.
- 2. A single-factor experiment was designed to determine the parameter ranges: the diameter of the circulating air inlet was 15~25 mm, the number of layers of the circulating air duct was 11~13, the diameter of the bottom ventilation opening was 4~6 mm, and the number of ventilation openings was 5~7. The first three factors were selected for response surface optimization experiments, and the optimization function of the Design Expert 13 software was used to determine the optimal parameter combination as a circulating air inlet diameter of 20 mm, 13 circulating air layers, a bottom ventilation opening diameter of 6 mm, and 7 ventilation openings.
- 3. The optimized circulation silo was subjected to simulation, and the results were compared with the original structural data. The relative standard deviation *CV* of the circulation grain storage silo decreased from 0.6188 to 0.4693, decreasing by 24.1%.

This study demonstrated a way to significantly improve the uniformity of airflow in corn storage silos. A modified design expanded the influence range of the grain pile during ventilation, reduced the accumulation of moisture and heat caused by poor airflow, and prevented problems such as excessive local moisture or insufficient moisture. This helped to maintain stable and uniform moisture levels throughout the entire silo and ensures consistent grain quality. In addition, the structural optimization method used in this study, which combines computational fluid dynamics (CFD) simulation with response surface optimization, not only is applicable to corn silos, but it also provides a referenceable technical approach and practical guidance for the design of ventilation systems in storage facilities for other granular materials such as wheat, rice, wood pellet particles, *etc*.

ACKNOWLEDGMENTS

This research was supported by the Joint Guidance Project of Natural Science Foundation of Heilongjiang Province (LH2023C059) and the National Fund Cultivation Project of Jiamusi University (JMSUGPZR2023-014).

REFERENCES CITED

- Abbouda, S. K., Chung, D. S., Seib, P. A., and Song, A. (1992). "Heat and mass transfer in stored milo. part i. heat transfer model," *Transactions of the ASAE* 35(5), 1569-1573. https://doi.org/10.13031/2013.28769
- Chen, S. Y., Wang, Z. X., Wu, W. F., and Liu, C. S. (2024). "Simulation analysis of circulating ventilation and longitudinal ventilation in corn storage silo based on EDEM-fluent," *Transactions of the Chinese Society of Agricultural Engineering* 40(06), 40-49. https://doi.org/10.11975/j.issn.1002-6819.202310157
- Gao, L. W., Xu, S. H., Li, Z. M., Cheng, S. K., Yu, W., Zhang, Y. G., and Wu C. (2016). "Research on the characteristics and mitigation potential of post-harvest losses of major crops in China," *Transactions of the Chinese Society of Agricultural Engineering* 32(23), 1-11. https://doi.org/10.11975/j.issn.1002-6819.2016.23.001
- Garg, D., and Maier, D. E. (2006). "Modeling non-uniform airflow distribution in large grain silos using Fluent," in: 9th International Working Conference on Stored Product Protection
- Gong, Z. L., Wang, P. K., Li, D. P., Yi, Z. P., Liu, H., Wen, T., and Zhang, Z. (2021). "Thermal field analysis and structural optimization of multi-temperature zone belt dryer," *Transactions of the Chinese Society of Agricultural Engineering* 37(18), 40-47. https://doi.org/10.11975/j.issn.1002-6819.2021.18.005
- Li, J., Song, C. F., Yang, D., and Shi, T. Y. (2023). "The influence of branch air duct height on radial ventilation in shallow round silos," *Chinese Journal of Food Science and Technology*, 38(04), 7-14. https://doi.org/10.3969/j.issn.1003-0174.2023.04.003
- Li, J. B., Wang, Y. C., Liu, J. C., Yang, T., and Yang, K. M. (2023). "Simulation study on the impact of a new ventilation network on the ventilation effect of open-type silo," *Grain and Food Science Technology* 31(01), 189-195. DOI: https://doi.org/10.16210/j.cnki.1007-7561.2023.01.024
- Li, T., Jin, S. P., Huang, S. Y., and Liu, W. (2013). "Comparative study on evaluation indicators of uniformity of flow field velocity distribution and its application," *Thermal Power Generation* 42(11), 60-63+92. https://doi.org/10.3969/j.issn.1002-3364.2013.11.060

- Liang, Y. W., Jin Y. F., Wang W., Gao J. J., Tang Z. K., Chen L. E., and Zhu M. K. (2021). "Comparison of horizontal and vertical ventilation cooling and moisture retention efficiency in high-growth shed," *Grain Storage* 50(06), 25-30. https://doi.org/10.3969/j.issn.1000-6958.2021.06.006
- Liu, L. Y., Wang, Y. C., Zhao, D. R., Wang, X. G., Lou Z., and Liu, F. J. (2020). "Analysis of airflow field in mechanical ventilation steel mesh-type wheat drying and storage silos used by farmers," *Transactions of the Chinese Society of Agricultural Engineering* 36(02), 312-319. https://doi.org/10.11975/j.issn.1002-6819.2020.02.036
- Luo, S. (2020). Numerical Simulation and Optimization Research on Air Flow Field and Temperature Field in Vertical Ventilated Pigsty Based on CFD, Master's Thesis, Jiangxi Agricultural University, China. https://link.cnki.net/DOI/10.27177/d.cnki. gjxnu.2020.000192
- Nwaizu, C., and Zhang, Q. (2021). "Computational modeling of heterogeneous pore structure and airflow distribution in grain aeration system," *Computers and Electronics in Agriculture* 188, article 106315. https://doi.org/10.1016/j.compag.2021.106315
- Qi, Y. K., Wang, Y. C., and Yu, X. J. (2019). "Comparative study on lateral and vertical ventilation in shallow round silos through numerical simulation," *Journal of Shandong University of Architecture and Technology*, 34(03), 50-56. https://doi.org/10.12077/sdjz.2019.03.008
- Qi, Y. K., Wang, Y. C., Yu, X. J., Wang, Y., and Kong, L. J. (2019). "Comparative study on lateral and vertical ventilation simulation when filling different grain heights in shallow round silos," *Journal of Henan University of Technology (Natural Science Edition)*, 40(04), 108-113. https://doi.org/10.16433/j.cnki.issn1673-2383.2019.04.019
- Ren, H. W., Li, J. P., Liu, Z. G., Yue, D. L., Zhang, F., and Li, Z. Z. (2012). "CFD numerical simulation of internal airflow field distribution in solar drying chamber," *Transactions of the Chinese Society of Agricultural Machinery* 43(S1), 235-238. https://doi.org/10.6041/j.issn.1000-1298.2012.S0.048
- Wang, M. G., and Zhao Z. Y. (2022). "Review of study on the mechanism of water transfer in the multi-filed coupling system of grain ecology for grain storage in bungalow granary," *Chinese Journal of Grain Science* 37(8), 28-35. https://doi.org/10.20048/j.cnki.issn.1003-0174.000409
- Wang, X. M., Wu, W. D., Yin, J., Zhang, Z.J., Wu, Z.D., and Yao, Q. (2019). "Research on temperature and humidity field change during corn bulk microbiological heating," *Journal of Agricultural Engineering* 35(03), 268-273. https://doi.org/10.11975/j.issn.1002-6819.2019.03.033
- Wang, Y. C., Yu, X. J., Shi, T. Y., and Yin J. (2020). "Research on the optimal humidity for lateral cooling and moisture retention ventilation of rice based on numerical prediction," *Chinese Journal of Food Science and Technology* 35(01), 113-120. https://doi.org/10.3969/j.issn.1003-0174.2020.01.019
- Wei, H., Yan, J. C., You, Z. Y., Wu, H. C., Xu, X. W., and Xie, H. X. (2021). "Simulation and analysis of peanut reversing ventilation drying performance," *Chinese Journal of Agricultural Mechanization* 42(10), 100-111. https://doi.org/10.13733/j.jcam.issn.2095-5553.2021.10.15
- Wu, S. Q., Ren, G. Y., Zhang, Y. L., Zhu, G. F., Bai, Y.S., Shi, J. F., and Duan, X. (2024). "Simulation and optimization of heat and moisture transfer during ventilation and drying of corn grain pile," *Transactions of the Chinese Society of Agricultural Engineering* 40(12), 264-275. https://doi.org/10.11975/j.issn.1002-6819.202402062

- Yan, J. C., Xie, H. X., Hu, Z. C., Wei, H., You, Z. Y., and Xue, H. B. (2015). "Simulation and process optimization of upward and downward reversing ventilating drying by fixed bed," *Transactions of the Chinese Society of Agricultural Engineering (Transactions of the CSAE)* 31(22), 292-300. https://doi.org/10.11975/j.issn.1002-6819.2015.22.040
- Yang, K. M., Dong, X. Q., Wang, Y. C., and Chu, F. J. (2024). "Simulation study on heat and moisture transfer in cross-flow drying aeration of bulk corn in a cone-bottom silo using natural and low-temperature air," *Journal of Food Process Engineering* 47(11), article e14774. https://doi.org/10.1111/jfpe.14774
- Yang, T., Zhang, X. L., Wang, Y. C., and Yang, K. M. (2022). "Simulation study on cooling effects of different ventilation forms in shallow round silo," *Grain Storage* 51(03), 1-7. https://doi.org/10.3969/j.issn.1000-6958.2022.03.001
- Yu, X. J., Wang, Y. C., and Qi, Y. K. (2019). "Simulation study on the ventilation effect of three different ventilation ducts in shallow round silos," *Food Science and Technology in China* 27(02), 61-66. https://doi.org/10.16210/j.cnki.1007-7561.2019.02.012
- Yu, X. J., Wang, Y. C., and Qi, Y. K. (2020). "Numerical simulation and analysis of lateral and vertical ventilation in high-rise flat-roof silos," *Journal of Shandong University of Architecture & Technology* 35(01), 64-70. https://doi.org/10.12077/sdjz.2020.01.010
- Zhao, Z., Yuan, Y. J., Li, L. F., Xu, Y. Y., Wang, Z. Q., and Xiong, F. K. (2023). "Molecular dynamics simulation of heat and mass transfer in the drying and aeration process of fruit and vegetable porous media in a cone-bottom silo using natural and low-temperature air," *Journal of Agricultural Engineering* 39(07), 285-294. https://doi.org/10.11975/j.issn.1002-6819.202207259
- Zhu, G. F., Bai, Y. S., Wang, S. L., Jiang, J. Q., Wu, S. Q., and Xie, Q. Z. (2023). "Simulation analysis and optimization of airflow field in corn dry storage integrated silo," *Transactions of the Chinese Society of Agricultural Machinery* 54(S1), 381-390. https://doi.org/10.6041/j.issn.1000-1298.2023.S1.041

Article submitted: July 26, 2025; Peer review completed: September 28, 2025; Revised version received: November 11, 2025; Accepted: November 13, 2025; Published: November 19, 2025.

DOI: 10.15376/biores.21.1.420-438